Contemporary Mathematics
Volume **141**, 1993

# Computational Biofluid Dynamics

CHARLES S. PESKIN AND DAVID M. MCQUEEN

ABSTRACT. The aims of this paper are (1) to give a general mathematical formulation to the central problem of biological fluid dynamics, which is the interaction of a viscous incompressible fluid with an elastic and possibly active material; (2) to describe a numerical method for the solution of the biofluid-dynamic problem; and (3) to illustrate both the mathematical formulation and the numerical method by considering the problem of blood flow in the heart. The work described in this paper is based on a mixed Eulerian-Lagrangian formulation. In computational terms this means that the fluid equations are solved by finite-difference methods on a fixed rectangular mesh, whereas the elasticity equations are modeled in terms of a network of moving material points connected by springs. Communication between Eulerian and Lagrangian variables is required in order to apply the elastic force to the fluid and to move the elastic material at the local fluid velocity. Such communication is mediated by an approximation to the Dirac delta function.

## 1. Introduction

Generally speaking, biological fluid dynamics involves the interaction of a viscous incompressible fluid with an elastic incompressible material. In some cases, the elastic material is *active*, which means that its elastic parameters may change with time in such a way that the material is capable of doing net work on the fluid.

The range of phenomena covered by this description is vast: it includes most (if not all) of the topics discussed at this conference. Some examples are the heart, the inner ear, the kidney, swimming, flight, filter feeding, blood flow in arteries, red cell transport through capillaries, and platelet aggregation during blood clotting.

---

1991 *Mathematics Subject Classification.* Primary 76, 92; Secondary 35, 65, 70.

This paper is in final form and no version of it will be submitted for publication elsewhere. Supported by the National Institutes of Health under research grant HL17859. Computation supported in part by the Minnesota Supercomputer Center.

Thus, it seems fair to say that *the* biofluid-dynamic problem is the interaction of a viscous incompressible fluid with a (possibly active) incompressible elastic material. The purpose of this paper, then, is to give a general mathematical formulation of the biofluid-dynamic problem and to describe an algorithm for its numerical solution.

Some, but not all, of the topics listed above have already been studied by the methods outlined here (Refs. 1–15). Perhaps one result of this conference will be the broader application of the computational approach to biofluid dynamics.

## 2. Equations of motion

It is a little-known fact that the equations of an incompressible *elastic body* can be written is such a way that they closely resemble the equations of an incompressible fluid (Refs. 16a, b). This "fluid-dynamic" formulation of incompressible elasticity is particularly useful when the body in question actually interacts with an incompressible fluid, for it then becomes possible to give a unified description of the composite system.

The fluid-dynamic formulation of the equations of incompressible elasticity may be obtained as follows. Let curvilinear coordinates $(q_1, q_2, q_3) = \mathbf{q}$ be introduced into an elastic substance in such a way that fixed $\mathbf{q}$ marks a material point. Let $\mathbf{X}(\mathbf{q}, t)$ be the position at time $t$ of the material point that carries the label $\mathbf{q}$. Let the set of all permissible values of $\mathbf{q}$ be denoted $\mathcal{Q}$. Then the region of space occupied by the elastic body at time $t$ is given by $\mathbf{X}(\mathcal{Q}, t) = \{\mathbf{x} : \mathbf{x} = \mathbf{X}(\mathbf{q}, t)$ for some $\mathbf{q} \in \mathcal{Q}\}$. We assume that this is some fixed region $\Omega$, independent of $t$. The function $\mathbf{X}(\ , t)$ maps $\mathcal{Q} \to \Omega$; we say that it describes the *configuration* of the elastic substance at time $t$. The description of the motion in terms of $\mathbf{X}(\mathbf{q}, t)$ is called a *Lagrangian* description. Later, we shall introduce an *Eulerian* description that is based on functions defined on $\Omega$ instead of $\mathcal{Q}$.

For simplicity, we consider the case in which $\mathcal{Q}$ and $\Omega$ are both the whole space $\mathcal{R}^3$, but we retain the notational distinction between $\mathcal{Q}$ and $\Omega$ for conceptual clarity. We assume that all disturbances of the elastic medium are sufficiently localized that (1) the integrals that appear below are finite, and (2) there are no boundary terms when we integrate by parts. This approach avoids the technical difficulties associated with boundary conditions and allows us to concentrate on the equations that hold in the interior of the elastic medium.

The local state of deformation of the elastic material is described by the $3 \times 3$ matrix $\partial\mathbf{X}/\partial\mathbf{q}$, with components $\partial X_i/\partial q_j$, $i, j = 1, 2, 3$. This matrix enters the theory in two ways. First, its determinant $J = \det(\partial\mathbf{X}/\partial\mathbf{q})$ gives the ratio of volume elements $d^3\mathbf{X} = J d^3\mathbf{q}$. Since the material in question is incompressible, this ratio is independent of time:

$$\det\left(\frac{\partial\mathbf{X}}{\partial\mathbf{q}}(\mathbf{q}, t)\right) = J(\mathbf{q}). \tag{1}$$

Second, the matrix $\partial\mathbf{X}/\partial\mathbf{q}$ determines the local density of elastic (potential)

energy. Thus

$$E_P(t) = \int_{\mathcal{Q}} \mathcal{E}(\frac{\partial \mathbf{X}}{\partial \mathbf{q}}(\mathbf{q},t),\mathbf{q},t))\, d^3\mathbf{q}, \tag{2}$$

where $E_P(t)$ is the potential energy of the system at time $t$ and where $\mathcal{E}$ is a function that characterizes the material (relative to the chosen system of curvilinear coordinates). Note that $\mathcal{E}$ has explicit position- and time-dependence in addition to that which it inherits from $\partial\mathbf{X}/\partial\mathbf{q}$. It is this explicit time-dependence that makes the material "active," as described in the Introduction. For a *passive* elastic material, this explicit time-dependence is not present, so the arguments of $\mathcal{E}$ are only $\partial\mathbf{X}/\partial\mathbf{q}$ and $\mathbf{q}$. (If the material is both passive and *homogeneous*, and if the coordinates are such that the homogeneity is manifest, then $\mathcal{E}$ is a function only of $\partial\mathbf{X}/\partial\mathbf{q}$.)

The kinetic energy of the system is, of course, given by the expression

$$E_K(t) = \frac{1}{2}\int_{\mathcal{Q}} m(\mathbf{q}) \left|\frac{\partial \mathbf{X}}{\partial t}(\mathbf{q},t)\right|^2 d^3\mathbf{q}, \tag{3}$$

where $m(\mathbf{q})$ is the local mass density with respect to the measure $d^3\mathbf{q}$. (Since the mass of a material element is conserved, $m$ is independent of time.)

Given the expressions for kinetic and potential energy together with the constraints on the motion of the material, we can derive the equations of motion from the *principle of least action*. (A limitation of this approach is that it fails to take viscosity into account; we shall put in the viscous terms later.)

The *action*, denoted $S$, over the time interval $(0,T)$ is defined as follows:

$$\begin{aligned} S &= \int_0^T [E_K(t) - E_P(t)]\, dt \\ &= \int_0^T \int_{\mathcal{Q}} \left\{ \frac{1}{2} m(\mathbf{q}) \left|\frac{\partial \mathbf{X}}{\partial t}(\mathbf{q},t)\right|^2 - \mathcal{E}\left[\frac{\partial \mathbf{X}}{\partial \mathbf{q}}(\mathbf{q},t),\mathbf{q},t\right]\right\} d^3\mathbf{q}\, dt. \end{aligned} \tag{4}$$

We seek $\mathbf{X}(\mathbf{q},t)$ to minimize $S$ subject to certain constraints. These constraints are (1) the motion is incompressible [eq. (1)], and (2) the initial and final configurations $\mathbf{X}(\ ,0)$ and $\mathbf{X}(\ ,T)$ are regarded as given. Note that the second constraint is artificial in the sense that we are rarely interested in the solution of an initial-final value problem. Nevertheless, it is part of the formulation of the principle of least action, which is used to obtain the equations of motion. These equations can then be solved with other boundary conditions, for example, the standard initial-value problem in which $\mathbf{X}(\ ,0)$ and $(\partial\mathbf{X}/\partial t)(\ ,0)$ are regarded as known.

Let $\mathbf{X}^{(0)}(\mathbf{q},t)$ be the solution to the optimization problem stated above, and consider the expansion

$$\mathbf{X}(\mathbf{q},t) = \mathbf{X}^{(0)}(\mathbf{q},t) + \epsilon\mathbf{X}^{(1)}(\mathbf{q},t) + \ldots. \tag{5}$$

This induces a corresponding expansion of $S$:

$$S = S^{(0)} + \epsilon S^{(1)} + \ldots. \tag{6}$$

Since $\mathbf{X}^{(0)}$ minimizes $S$, we require that $S^{(1)} = 0$ *for all* $\mathbf{X}^{(1)}$ *that are consistent with the constraints*. This leads to the equation

$$0 = \int_0^T \int_{\mathcal{Q}} \left( m \frac{\partial \mathbf{X}^{(0)}}{\partial t} \cdot \frac{\partial \mathbf{X}^{(1)}}{\partial t} - \sum_{i,j=1}^{3} \mathcal{E}_{ij}^{(0)} \frac{\partial X_i^{(1)}}{\partial q_j} \right) d^3q \, dt, \tag{7}$$

where

$$\mathcal{E}_{ij} = \frac{\partial \mathcal{E}}{\partial(\partial X_i/\partial q_j)} \left[ \frac{\partial \mathbf{X}}{\partial \mathbf{q}}(\mathbf{q}, t), \mathbf{q}, t \right], \tag{8}$$

and where the superscript 0 on $\mathcal{E}_{ij}$ means that it is to be evaluated at $\mathbf{X} = \mathbf{X}^{(0)}$. In equation (7), integrate the kinetic energy term by parts with respect to $t$ and the potential energy term by parts with respect to $q_j$. In both cases, the boundary terms drop out. In the case of the kinetic energy this is because of the formulation of the principle of least action as an initial-final value problem in which $\mathbf{X}(\ ,0)$ and $\mathbf{X}(\ ,T)$ are given. It follows from this that $\mathbf{X}^{(1)}(\ ,0) = \mathbf{X}^{(1)}(\ ,T) = 0$. In the case of the potential energy, the boundary terms drop out because of our explicit assumption that the disturbances are sufficiently localized for this to happen. The result is

$$0 = \int_0^T \int_{\mathcal{Q}} \sum_{i=1}^{3} \left[ m \frac{\partial^2 X_i^{(0)}}{\partial t^2} - \sum_{j=1}^{3} \left( \frac{d}{dq_j} \mathcal{E}_{ij}^{(0)} \right) \right] X_i^{(1)} \, d^3\mathbf{q} \, dt. \tag{9}$$

In the expression $\frac{d}{dq_j}\mathcal{E}_{ij}$, we use the notation of an ordinary derivative as a reminder that one must differentiate with respect to both occurrences of the argument $q_j$ [see eq. (8)]. Thus,

$$\frac{d\mathcal{E}_{ij}}{dq_j} = \sum_{k,l=1}^{3} \mathcal{E}_{ij,kl} \frac{\partial^2 X_k}{\partial q_l \partial q_j} + \frac{\partial \mathcal{E}_{ij}}{\partial q_j}, \tag{10}$$

where

$$\mathcal{E}_{ij,kl} = \frac{\partial^2 \mathcal{E}}{\partial(\partial X_i/\partial q_j)\partial(\partial X_k/\partial q_l)}. \tag{11}$$

Now let

$$f_i = \sum_{j=1}^{3} \frac{d\mathcal{E}_{ij}}{dq_j}. \tag{12}$$

Then equation (9) can be written as

$$0 = \int_0^T \int_{\mathcal{Q}} \left( m \frac{\partial^2 \mathbf{X}^{(0)}}{\partial t^2} - \mathbf{f}^{(0)} \right) \cdot \mathbf{X}^{(1)} \, d^3\mathbf{q} \, dt. \tag{13}$$

Recall, however, that $\mathbf{X}^{(1)}$ is not arbitrary. In particular, it must be consistent with the constraint of incompressibility. Thus, we cannot conclude that the coefficient of $\mathbf{X}^{(1)}$ is zero.

To proceed further, it is convenient to switch to Eulerian variables. These are functions of $(\mathbf{x}, t)$ where $\mathbf{x} \in \Omega$. For example, $\mathbf{u}(\mathbf{x}, t)$ is the velocity at time $t$ of the material point which happens to be at position $\mathbf{x}$ at time $t$. (Note the

absence of any information about *which* material point this is.) At time $t+dt$, a different material point occupies the position $\mathbf{x}$, so $\frac{\partial \mathbf{u}}{\partial t}(\mathbf{x},t)$ does not measure the physical acceleration of any material point. We can, on the other hand, define a function $\frac{D\mathbf{u}}{Dt}(\mathbf{x},t)$, which gives the acceleration at time $t$ of the material point which happens to be at position $\mathbf{x}$ at time $t$. The functions $\mathbf{u}(\mathbf{x},t)$ and $\frac{D\mathbf{u}}{Dt}(\mathbf{x},t)$ are implicitly defined as follows:

$$\mathbf{u}\left[\mathbf{X}^{(0)}(\mathbf{q},t),t\right] = \frac{\partial \mathbf{X}^{(0)}}{\partial t}(\mathbf{q},t), \tag{14}$$

$$\frac{D\mathbf{u}}{Dt}\left[\mathbf{X}^{(0)}(\mathbf{q},t),t\right] = \frac{\partial^2 \mathbf{X}^{(0)}}{\partial t^2}(\mathbf{q},t). \tag{15}$$

Differentiating equation (14) with respect to time, one can show that

$$\frac{D\mathbf{u}}{Dt} = \frac{\partial \mathbf{u}}{\partial t} + \mathbf{u}\cdot\nabla\mathbf{u}. \tag{16}$$

By analogy with the Eulerian velocity $\mathbf{u}(\mathbf{x},t)$, we can introduce an Eulerian vector field $\mathbf{v}(\mathbf{x},t)$ corresponding to the Lagrangian perturbation $\mathbf{X}^{(1)}(\mathbf{q},t)$. The implicit definition of $\mathbf{v}(\mathbf{x},t)$ is as follows:

$$\mathbf{v}\left[\mathbf{X}^{(0)}(\mathbf{q},t),t\right] = \mathbf{X}^{(1)}(\mathbf{q},t). \tag{17}$$

In this definition, note that $\mathbf{v}$ is evaluated at the unperturbed position $\mathbf{X}^{(0)}(\mathbf{q},t)$.

The Eulerian form of the incompressibility constraint can be obtained as follows. Let $\partial\mathbf{u}/\partial\mathbf{x}$ be the $3\times 3$ matrix with elements $\partial u_i/\partial x_j$. Differentiating equation (14) with respect to $\mathbf{q}$ yields the matrix equation

$$\frac{\partial \mathbf{u}}{\partial \mathbf{x}}\frac{\partial \mathbf{X}^{(0)}}{\partial \mathbf{q}} = \frac{\partial^2 \mathbf{X}^{(0)}}{\partial \mathbf{q}\partial t}, \tag{18}$$

or

$$\frac{\partial \mathbf{u}}{\partial \mathbf{x}} = \frac{\partial^2 \mathbf{X}^{(0)}}{\partial \mathbf{q}\partial t}\left(\frac{\partial \mathbf{X}^{(0)}}{\partial \mathbf{q}}\right)^{-1}. \tag{19}$$

It follows that

$$\begin{aligned}\nabla\cdot\mathbf{u} &= \operatorname{trace}\left(\frac{\partial \mathbf{u}}{\partial \mathbf{x}}\right) = \operatorname{trace}\left[\frac{\partial^2 \mathbf{X}^{(0)}}{\partial \mathbf{q}\partial t}\left(\frac{\partial \mathbf{X}^{(0)}}{\partial \mathbf{q}}\right)^{-1}\right] \\ &= \frac{d}{dt}\log\det\left(\frac{\partial \mathbf{X}^{(0)}}{\partial \mathbf{q}}\right) = \frac{d}{dt}\log\left[J^{(0)}(\mathbf{q})\right] \\ &= 0,\end{aligned} \tag{20}$$

where we have used the general formula for the derivative of a determinant:

$[\log \det A(t)]' = \text{trace}[A'(t)A^{-1}(t)]$. Similarly,

$$\begin{aligned}\nabla \cdot \mathbf{v} &= \text{trace}\left(\frac{\partial \mathbf{v}}{\partial \mathbf{x}}\right) = \text{trace}\left[\frac{\partial \mathbf{X}^{(1)}}{\partial \mathbf{q}}\left(\frac{\partial \mathbf{X}^{(0)}}{\partial \mathbf{q}}\right)^{-1}\right] \\ &= \lim_{\epsilon \to 0} \text{trace}\left[\frac{\partial^2 \mathbf{X}}{\partial \mathbf{q} \partial \epsilon}\left(\frac{\partial \mathbf{X}}{\partial \mathbf{q}}\right)^{-1}\right] \\ &= \lim_{\epsilon \to 0} \frac{\partial}{\partial \epsilon} \log\left[\det\left(\frac{\partial \mathbf{X}}{\partial \mathbf{q}}\right)\right] \\ &= \lim_{\epsilon \to 0} \frac{\partial}{\partial \epsilon} \log J(\mathbf{q}) = 0, \end{aligned} \tag{21}$$

since $J(\mathbf{q})$ is independent of $\epsilon$. (All motions under consideration are consistent with the incompressibility constraint.)

Formulas for the conversion between Lagrangian and Eulerian variables can also be expressed in terms of the Dirac delta function. In particular, we shall make use of the following:

$$\mathbf{X}^{(1)}(\mathbf{q},t) = \int_\Omega \mathbf{v}(\mathbf{x},t)\, \delta^3\left[\mathbf{x} - \mathbf{X}^{(0)}(\mathbf{q},t)\right]\, d^3\mathbf{x} \tag{22}$$

$$\frac{\partial^2 \mathbf{X}^{(0)}}{\partial t^2}(\mathbf{q},t) \cdot \mathbf{X}^{(1)}(\mathbf{q},t) = \int_\Omega \frac{D\mathbf{u}}{Dt}(\mathbf{x},t) \cdot \mathbf{v}(\mathbf{x},t)\, \delta^3\left[\mathbf{x} - \mathbf{X}^{(0)}(\mathbf{q},t)\right]\, d^3\mathbf{x}. \tag{23}$$

Equation (22) is equivalent to equation (17), and equation (23) is equivalent to the result obtained by taking the dot product of equations (15) and (17).

Finally, we introduce the mass density $\rho(\mathbf{x},t)$ and the Eulerian force density $\mathbf{F}(\mathbf{x},t)$ according to the following definitions:

$$\rho(\mathbf{x},t) = \int_Q m(\mathbf{q})\, \delta^3\left[\mathbf{x} - \mathbf{X}^{(0)}(\mathbf{q},t)\right]\, d^3\mathbf{q}, \tag{24}$$

$$\mathbf{F}(\mathbf{x},t) = \int_Q \mathbf{f}^{(0)}(\mathbf{q},t)\, \delta^3\left[\mathbf{x} - \mathbf{X}^{(0)}(\mathbf{q},t)\right]\, d^3\mathbf{q}. \tag{25}$$

Note that the integrals in equations (24) and (25) are to be done with respect to the variable $\mathbf{q} \in Q$, whereas the integrals in equations (22) and (23) are to be done with respect to $\mathbf{x} \in \Omega$. It is easy to check that $\rho(\mathbf{x},t)$ satisfies the continuity equation $\partial\rho/\partial t + \mathbf{u} \cdot \nabla\rho = 0$. [Since $\nabla \cdot \mathbf{u} = 0$, this is equivalent to $\partial\rho/\partial t + \nabla \cdot (\rho\mathbf{u}) = 0$.]

Having set up all of this Eulerian apparatus, we are now ready to convert

equation (13) to Eulerian form. This is done as follows:

$$
\begin{aligned}
0 &= \int_0^T \int_{\mathcal{Q}} m(\mathbf{q}) \frac{\partial^2 \mathbf{X}^{(0)}}{\partial t^2}(\mathbf{q},t) \cdot \mathbf{X}^{(1)}(\mathbf{q},t)\, d^3\mathbf{q}\, dt \\
&\quad - \int_0^T \int_{\mathcal{Q}} \mathbf{f}^{(0)}(\mathbf{q},t) \cdot \mathbf{X}^{(1)}(\mathbf{q},t)\, d^3\mathbf{q}\, dt \\
&= \int_0^T \int_{\mathcal{Q}} \int_{\Omega} m(\mathbf{q}) \frac{D\mathbf{u}}{Dt}(\mathbf{x},t) \cdot \mathbf{v}(\mathbf{x},t)\, \delta^3\left[\mathbf{x} - \mathbf{X}^{(0)}(\mathbf{q},t)\right]\, d^3\mathbf{x}\, d^3\mathbf{q}\, dt \\
&\quad - \int_0^T \int_{\mathcal{Q}} \int_{\Omega} \mathbf{f}^{(0)}(\mathbf{q},t) \cdot \mathbf{v}(\mathbf{x},t)\, \delta^3\left[\mathbf{x} - \mathbf{X}^{(0)}(\mathbf{q},t)\right]\, d^3\mathbf{x}\, d^3\mathbf{q}\, dt \\
&= \int_0^T \int_{\Omega} \rho(\mathbf{x},t) \frac{D\mathbf{u}}{Dt}(\mathbf{x},t) \cdot \mathbf{v}(\mathbf{x},t)\, d^3\mathbf{x}\, dt - \int_0^T \int_{\Omega} \mathbf{F}(\mathbf{x},t) \cdot \mathbf{v}(\mathbf{x},t)\, d^3\mathbf{x}\, dt \\
&= \int_0^T \int_{\Omega} \left(\rho \frac{D\mathbf{u}}{Dt} - \mathbf{F}\right) \cdot \mathbf{v}\, d^3\mathbf{x}\, dt. \qquad (26)
\end{aligned}
$$

Equation (26) is required to hold for all $\mathbf{v}$ such that $\nabla \cdot \mathbf{v} = 0$, $\mathbf{v}(\mathbf{x},0) = 0$, and $\mathbf{v}(\mathbf{x},T) = 0$. This will be true if and only if

$$\rho \frac{D\mathbf{u}}{Dt} - \mathbf{F} = -\nabla p \qquad (27)$$

for some scalar $p$, which is conventionally called the pressure. To prove that equation (27) $\Longrightarrow$ equation (26), one simply notes that

$$-\int_{\Omega} \nabla p \cdot \mathbf{v}\, d^3\mathbf{x} = \int_{\Omega} p(\nabla \cdot \mathbf{v})\, d^3\mathbf{x} = 0, \qquad (28)$$

since $\nabla \cdot \mathbf{v} = 0$. To prove the converse is only a little more difficult. First, let $p$ be defined as the solution of the Poisson equation

$$-\nabla^2 p = \nabla \cdot \left(\rho \frac{D\mathbf{u}}{Dt} - \mathbf{F}\right), \qquad (29)$$

and let

$$\mathbf{w} = \left(\rho \frac{D\mathbf{u}}{Dt} - \mathbf{F}\right) + \nabla p. \qquad (30)$$

It follows from equation (29) that

$$\nabla \cdot \mathbf{w} = 0. \qquad (31)$$

Therefore, we may choose

$$\mathbf{v}(\mathbf{x},t) = \phi(t)\mathbf{w}(\mathbf{x},t), \qquad (32)$$

where $\phi(0) = \phi(T) = 0$ and $\phi(t) > 0$ for $0 < t < T$. Now since $\int_\Omega \mathbf{v} \cdot \nabla p \, d\mathbf{x} = 0$, as shown above, we have

$$0 = \int_0^T \int_\Omega \rho \left( \frac{D\mathbf{u}}{Dt} - \mathbf{F} \right) \cdot \mathbf{v} \, d^3\mathbf{x} \, dt$$
$$= \int_0^T \int_\Omega \mathbf{w} \cdot \mathbf{v} \, d^3\mathbf{x} \, dt = \int_0^T \phi(t) \int_\Omega |\mathbf{w}(\mathbf{x}, t)|^2 \, d^3\mathbf{x} \, dt. \tag{33}$$

It follows [since $\phi > 0$ in the interior of $(0, T)$] that $\mathbf{w} = 0$ and hence [see eq. (30)] that $\rho \frac{D\mathbf{u}}{Dt} - \mathbf{F} = -\nabla p$, as claimed.

We may now collect together in one place the system of equations for the incompressible elastic material. In so doing, we shall arbitrarily add a viscous term $\mu \nabla^2 \mathbf{u}$, since viscosity was omitted from the foregoing derivation. (Also, we now drop the superscript 0 which previously distinguished the true motion from the perturbed motion.) The equations are

$$\rho \left( \frac{\partial \mathbf{u}}{\partial t} + \mathbf{u} \cdot \nabla \mathbf{u} \right) + \nabla p = \mu \nabla^2 \mathbf{u} + \mathbf{F}, \tag{34}$$

$$\nabla \cdot \mathbf{u} = 0, \tag{35}$$

$$\rho(\mathbf{x}, t) = \int_{\mathcal{Q}} m(\mathbf{q}) \delta^3 [\mathbf{x} - \mathbf{X}(\mathbf{q}, t)] \, d^3\mathbf{q}, \tag{36}$$

$$\mathbf{F}(\mathbf{x}, t) = \int_{\mathcal{Q}} \mathbf{f}(\mathbf{q}, t) \delta^3 [\mathbf{x} - \mathbf{X}(\mathbf{q}, t)] \, d^3\mathbf{q}, \tag{37}$$

$$\frac{\partial \mathbf{X}}{\partial t}(\mathbf{q}, t) = \int_\Omega \mathbf{u}(\mathbf{x}, t) \delta^3 [\mathbf{x} - \mathbf{X}(\mathbf{q}, t)] \, d^3\mathbf{x}, \tag{38}$$

$$f_i = \sum_{j=1}^{3} \frac{d\mathcal{E}_{ij}}{dq_j}. \tag{39}$$

These equations provide a mixed Eulerian-Lagrangian description of the motion. Equations (34) and (35) may be recognized as the Navier-Stokes equations of a viscous incompressible fluid that carries a nonuniform mass density $\rho(\mathbf{x}, t)$ and that moves under the influence of an external force density $\mathbf{F}(\mathbf{x}, t)$. Here, however, the force density is not external, but arises from the elastic stresses in the material itself. Since these stresses are determined by the configuration of the elastic material, their computation requires a Lagrangian description of the motion. Equation (39) gives the formula for the Lagrangian force density $\mathbf{f}$ in terms of the elastic potential energy density $\mathcal{E}$ [see also eqs. (8), (10), and (11), which define $\mathcal{E}_{ij}$ and $d\mathcal{E}_{ij}/dq_j$].

Equations (36)–(38) are the interaction equations which connect the Lagrangian and Eulerian variables. All three of these are integral transformations involving the kernel $\delta^3[\mathbf{x} - \mathbf{X}(\mathbf{q}, t)]$. In the first two cases, however, the integration is with respect to $\mathbf{q}$ whereas in the third it is with respect to $\mathbf{x}$. Although the interaction equations could be rewritten in such a way as to avoid the use

of the Dirac delta function, the particular formulation given here is useful because it leads directly to an effective numerical scheme, as explained in the next section.

As stated at the beginning of this section, the formulation given here adapts itself to the situation in which an elastic incompressible material interacts with a viscous incompressible fluid. In that case, we can simply think of the fluid as a part of the elastic material in which the elastic energy density $\mathcal{E}$ happens to be zero, and the equations given above can be used unchanged. (Alternatively, one can think of the elastic material as a part of the fluid where additional stresses are applied; the equations are the same whichever way we happen to think of it.)

When the system is partly fluid, it should be noted that the Lagrangian description of the fluid part of the system is unnecessary, provided that the fluid in question is homogeneous, since the great virtue of a homogeneous fluid is that it consists of "interchangeable parts," and the Lagrangian label $\mathbf{q}$ is therefore irrelevant. We can exploit this by confining the Lagrangian description to the elastic part of the system. This means that $\mathbf{X}(\mathcal{Q}, t)$, the image of $\mathcal{Q}$ under the map $\mathbf{q} \to \mathbf{X}(\mathbf{q}, t)$, is no longer the entire space $\Omega$ but only the part of $\Omega$ that is occupied by the elastic material. Of course, this part can change with time as the elastic material moves about in the fluid. Under these circumstances, we must modify equation (36), since we are no longer keeping track of the mass of the fluid in Lagrangian fashion.

Let $\rho_0$ be the constant mass density of the fluid and let $m(\mathbf{q})d^3\mathbf{q}$ be reinterpreted as the *additional mass* of the element $d^3\mathbf{q}$ of the elastic material. By additional mass is meant the difference between the actual mass and the mass of the fluid displaced by the element in question. (Note that the additional mass can be negative.) Then the total mass density $\rho(\mathbf{x}, t)$ is given by

$$\rho(\mathbf{x}, t) = \rho_0 + \int_{\mathcal{Q}} m(\mathbf{q})\delta^3 \left[\mathbf{x} - \mathbf{X}(\mathbf{q}, t)\right] d^3\mathbf{q}, \tag{40}$$

which replaces equation (36). An important special case is the situation in which the elastic material is neutrally buoyant in the fluid. Then $m(\mathbf{q}) = 0$, and $\rho(\mathbf{x}, t) = \rho_0$, independent of $\mathbf{x}$ and $t$.

As a further generalization of equation (34)–(39), consider the case in which the elastic material is confined to a surface. We refer to such a surface as an immersed elastic boundary. There are many biological examples in which an elastic membrane interacts with a viscous incompressible fluid, for example, heart valve leflets and the basilar membrane of the inner ear, as well as the fins of fish and the wings of birds and bats. In the case of an immersed elastic boundary, the Lagrangian part of the formulation becomes two-dimensional whereas the Eulerian part remains three-dimensional. The interaction equations now take

the form

$$\rho(\mathbf{x},t) = \rho_0 + \int_{\mathcal{Q}} m(q_1,q_2)\delta^3[\mathbf{x}-\mathbf{X}(q_1,q_2,t)]\,dq_1dq_2, \tag{41}$$

$$\mathbf{F}(\mathbf{x},t) = \int_{\mathcal{Q}} \mathbf{f}(q_1,q_2,t)\delta^3[\mathbf{x}-\mathbf{X}(q_1,q_2,t)]\,dq_1dq_2, \tag{42}$$

$$\frac{\partial \mathbf{X}}{\partial t}(q_1,q_2,t) = \int_{\Omega} \mathbf{u}(\mathbf{x},t)\delta^3[\mathbf{x}-\mathbf{X}(q_1,q_2,t)]\,d\mathbf{x} \tag{43}$$

[although it is often the case that the mass of the membrane may be neglected, in which case eq. (41) reduces to $\rho(\mathbf{x},t) = \rho_0$.] Note that equations (41) and (42) involve the three-dimensional delta-function, but only a two-dimensional integral. Thus, the result is singular with the same type of singularity as a one-dimensional delta-function. In particular, the force density $\mathbf{F}(\mathbf{x},t)$ is infinite on the immersed elastic boundary and zero everywhere else, but its integral is always finite. Indeed, let $\Omega'$ be any subregion of $\Omega$. Then

$$\begin{aligned}\int_{\Omega'} \mathbf{F}(\mathbf{x},t)\,d^3\mathbf{x} &= \int_{\mathcal{Q}} \mathbf{f}(q_1,q_2,t) \int_{\Omega'} \delta^3[\mathbf{x}-\mathbf{X}(q_1,q_2,t)]\,d^3\mathbf{x}dq_1dq_2 \\ &= \int_{\mathcal{Q}} \mathbf{f}(q_1,q_2,t) \left\{ \begin{array}{ll} 1, & \mathbf{X}(q_1,q_2,t) \in \Omega' \\ 0, & \text{otherwise} \end{array} \right\} dq_1dq_2 \\ &= \int_{\mathcal{Q}'(t)} \mathbf{f}(q_1,q_2,t)\,dq_1dq_2, \end{aligned} \tag{44}$$

where

$$\mathcal{Q}'(t) = \{q_1,q_2 : \mathbf{X}(q_1,q_2,t) \in \Omega'\}\,. \tag{45}$$

In other words, the force on the region $\Omega'$ comes from that part of the immersed elastic boundary that lies in $\Omega'$.

In summary, we have derived a mixed Eulerian-Lagrangian formulation of the equations of incompressible elasticity. This formulation uses the Dirac delta-function to make the connection between the two modes of description of the motion, and it lends itself well to the description of a variety of situations in which an elastic material interacts with a viscous incompressible fluid.

## 3. Numerical method

In this section we describe a method for the numerical solution of equations (34)–(39). Recall that these equations involve two conceptually distinct spatial domains: $\Omega$, the domain of the Eulerian variables, and $\mathcal{Q}$, the domain of the Lagrangian variables. For simplicity, we made the assumption that each of these domains was coincident with $\mathcal{R}^3$, and we retain that assumption here. (In practice, though, we replace $\mathcal{R}^3$ by a periodic domain which has the advantage of being finite while retaining the translation-invariant character of $\mathcal{R}^3$.)

Let $\Omega$ be represented by the cubic lattice of points

$$\Omega_h = \left\{\mathbf{x} \in \Omega : \mathbf{x} = \mathbf{j}h \quad \text{for some } \mathbf{j} \in \mathcal{Z}^3\right\}, \tag{46}$$

where $h$ is a positive parameter called the mesh width and where $\mathcal{Z}$ denotes the set of all integers [so $\mathcal{Z}^3$ is the set of all ordered triples of integers $(j_1, j_2, j_3)$]. Similarly, let $\mathcal{Q}_h$ be the cubic lattice

$$\mathcal{Q}_h = \{\mathbf{q} \in \mathcal{Q} : \mathbf{q} = \mathbf{k}\alpha h \quad \text{for some } \mathbf{k} \in \mathcal{Z}^3\}, \tag{47}$$

where $\alpha$ is some fixed constant independent of $h$, so that the mesh widths of the Eulerian and Lagrangian grids are proportional as $h \to 0$.

The grids $\Omega_h$ and $\mathcal{Q}_h$ are, of course, fixed in their respective domains, but the set $\mathbf{X}(\mathcal{Q}_h, t)$, which is the image of $\mathcal{Q}_h$ under the map $\mathbf{q} \to \mathbf{X}(\mathbf{q}, t)$, is an array of points in $\Omega$; they are not restricted to the cubic lattice $\Omega_h$ on which the Eulerian variables (such as velocity and pressure) are defined. This immediately brings up the problem of communication between the Lagrangian and Eulerian variables.

The key to such communication is contained in the interaction equations, equations (36) to (38). Recall that these are integral transformations with the kernel $\delta^3[\mathbf{x} - \mathbf{X}(\mathbf{q}, t)]$. For computational purposes we replace the integral by a sum and the kernel by $\delta_h^3[\mathbf{x} - \mathbf{X}(\mathbf{q}, t)]$, where $\delta_h^3$ is defined as follows:

$$\delta_h^3(\mathbf{x}) = \delta_h(x_1)\delta_h(x_2)\delta_h(x_3), \tag{48}$$

where $\mathbf{x} = (x_1, x_2, x_3)$ and where

$$\delta_h(x) = \begin{cases} \frac{1}{4h}(1 + \cos\frac{\pi x}{2h}) & |x| \le 2h \\ 0 & |x| \ge 2h \end{cases} \tag{49}$$

The motivation for this particular choice of $\delta_h$ is discussed in References 1 and 2. Thus, we are led to the discrete interaction equations

$$\rho(\mathbf{x}, t) = \sum_{\mathbf{q} \in \mathcal{Q}_h} m(\mathbf{q})\delta_h^3[\mathbf{x} - \mathbf{X}(\mathbf{q}, t)](\alpha h)^3, \tag{50}$$

$$\mathbf{F}(\mathbf{x}, t) = \sum_{\mathbf{q} \in \mathcal{Q}_h} \mathbf{f}(\mathbf{q}, t)\delta_h^3[\mathbf{x} - \mathbf{X}(\mathbf{q}, t)](\alpha h)^3, \tag{51}$$

$$\mathbf{U}(\mathbf{q}, t) = \sum_{\mathbf{x} \in \Omega_h} \mathbf{u}(\mathbf{x}, t)\delta_h^3[\mathbf{x} - \mathbf{X}(\mathbf{q}, t)]h^3, \tag{52}$$

where we have introduced the notation $\mathbf{U} = \partial\mathbf{X}/\partial t$. Note that equations (50) and (51) are used only for $\mathbf{x} \in \Omega_h$ and that equation (52) is used only for $\mathbf{q} \in \mathcal{Q}_h$.

One of the properties of the function $\delta_h^3$ defined above is that

$$\sum_{\mathbf{x} \in \Omega_h} \delta_h^3(\mathbf{x} - \mathbf{X})h^3 = 1 \tag{53}$$

for all $\mathbf{X} \in \Omega$ (not just for $\mathbf{X} \in \Omega_h$). Because of this property (and because $\delta_h^3 \ge 0$), equation (52) defines $\mathbf{U}(\mathbf{q}, t)$ as a weighted average of $\mathbf{u}(\mathbf{x}, t)$. The average is taken over the $4 \times 4 \times 4$ sublattice of $\Omega_h$ which is most nearly centered on the point $\mathbf{X}(\mathbf{q}, t)$. Thus, we may describe equation (52) as an interpolation formula.

Something a little more complicated is going on in the case of equations (50) and (51). This is because

$$\sum_{\mathbf{q}' \in \mathcal{Q}_h} \delta_h^3[\mathbf{x} - \mathbf{X}(\mathbf{q}', t)](\alpha h)^3 \neq 1, \tag{54}$$

not even approximately. To see the reason for this, recall that

$$\int_{\mathcal{Q}} \delta^3[\mathbf{x} - \mathbf{X}(\mathbf{q}', t)]\, d^3\mathbf{q}' = \frac{1}{J(\mathbf{q})}, \tag{55}$$

where $\mathbf{x}$ and $\mathbf{q}$ are related by $\mathbf{x} = \mathbf{X}(\mathbf{q}, t)$. Thus the sum in equation (54) is an approximation to $1/J(\mathbf{q})$, which is independent of time but is not necessarily equal to 1. It follows that we cannot (in general) interpret $\rho$ as the weighted average of $m$, nor can we interpret $\mathbf{F}$ as the weighted average of $\mathbf{f}$. [This distinction becomes even more clear in the case of an immersed elastic boundary; see eqs. (41)–(43). There, $m$ and $\mathbf{f}$ are finite quantities, but $\rho$ and $\mathbf{F}$ are infinite in the continuous formulation, and $O(h^{-1})$ in the corresponding discrete formulation.]

The correct mathematical interpretation of the operation defined by equation (51) is that it is the adjoint of the operation defined by equation (52). [The operation in eq. (50) is essentially the same as that in eq. (51), the only difference being that it is applied to scalars instead of vectors.) To see this, define the inner product of two functions defined on $\Omega_h$ as follows:

$$(\mathbf{u}, \mathbf{v})_{\Omega_h} = \sum_{\mathbf{x} \in \Omega_h} \mathbf{u}(\mathbf{x}) \cdot \mathbf{v}(\mathbf{x}) h^3. \tag{56}$$

Similarly, define

$$(\mathbf{f}, \mathbf{g})_{\mathcal{Q}_h} = \sum_{\mathbf{q} \in \mathcal{Q}_h} \mathbf{f}(\mathbf{q}) \cdot \mathbf{g}(\mathbf{q})(\alpha h)^3. \tag{57}$$

Note that

$$\begin{aligned}(\mathbf{F}, \mathbf{u})_{\Omega_h} &= \sum_{\mathbf{x} \in \Omega_h} \sum_{\mathbf{q} \in \mathcal{Q}_h} \mathbf{u}(\mathbf{x}, t) \cdot \mathbf{f}(\mathbf{q}, t) \delta_h^3[\mathbf{x} - \mathbf{X}(\mathbf{q}, t)](\alpha h)^3 h^3 \\ &= (\mathbf{f}, \mathbf{U})_{\mathcal{Q}_h}. \end{aligned} \tag{58}$$

If we call the interpolation operator $S$, so that $\mathbf{U} = S\mathbf{u}$, then equation (58) reads

$$(\mathbf{F}, \mathbf{u})_{\Omega_h} = (\mathbf{f}, S\mathbf{u})_{\mathcal{Q}_h}, \tag{59}$$

which shows that

$$\mathbf{F} = S^* \mathbf{f}, \tag{60}$$

where $S^*$ denotes the adjoint of $S$.

Incidentally, the identity given by equation (58) states that the total power is the same whether we calculate it in Eulerian or in Lagrangian form. This is certainly true in the continuous formulation of the problem, but it is only true in the discrete formulation because we use the same function $\delta_h^3$ in equation (51) as in (52).

We now turn to the discretization of equation (39), which is the Lagrangian computation of the elastic force density from the instantaneous configuration of the elastic material. Let the difference operators $D^{\pm}$ be defined as follows:

$$(D^{+}\phi)(\theta) = \frac{\phi(\theta + \Delta\theta) - \phi(\theta)}{\Delta\theta}, \tag{61}$$

$$(D^{-}\phi)(\theta) = \frac{\phi(\theta) - \phi(\theta - \Delta\theta)}{\Delta\theta}, \tag{62}$$

and let a subscript on $D^{\pm}$ denote the independent variable that is involved in the differencing operator (all other independent variables being held constant). Note that

$$\sum_{\theta} \phi(\theta)(D^{+}\psi)(\theta)\Delta\theta = -\sum_{\theta}(D^{-}\phi)(\theta)\psi(\theta)\Delta\theta, \tag{63}$$

where the sum is over the one-dimensional lattice of points of the form $\theta = j\Delta\theta$, where $j$ is any integer. This "summation by parts" identity is easily proved by shifting indices as needed.

Given the operators $D^{+}$ and $D^{-}$, we discretize equation (39) as follows:

$$f_i = \sum_{j=1}^{3} D^{-}_{q_j} \mathcal{E}_{ij}(\cdots D^{+}_{q_l} X_k \cdots, \mathbf{q}, t). \tag{64}$$

Here, the function $\mathcal{E}_{ij}$ is the same as in the continuous case [eq. (8)], but the argument $\partial X_k/\partial q_l$ has been evaluated at $D^{+}_{q_l} X_k$.

We remark that equation (64) may be derived by considering the variation of the discrete elastic energy function

$$E = \sum_{\mathbf{q}\in\mathcal{Q}_h} \mathcal{E}(\cdots D^{+}_{q_j} X_i \cdots, \mathbf{q}, t)(\alpha h)^3. \tag{65}$$

As above, $\mathcal{E}$ is the continuous energy density function, but its argument $\partial X_i/\partial q_j$ is evaluated at $D^{+}_{q_j} X_i$. Now consider a small change in configuration and evaluate the corresponding change in $E$ to first order:

$$\begin{aligned} dE &= \sum_{\mathbf{q}\in\mathcal{Q}_h} \sum_{i,j=1}^{3} \mathcal{E}_{ij}(\cdots D^{+}_{q_l} X_k \cdots, \mathbf{q}, t)(D^{+}_{q_j} dX_i)(\alpha h)^3 \\ &= -\sum_{\mathbf{q}\in\mathcal{Q}_h} \sum_{i,j=1}^{3} (D^{-}_{q_j} \mathcal{E}_{ij}(\cdots D^{+}_{q_l} X_k \cdots, \mathbf{q}, t) dX_i (\alpha h)^3, \end{aligned} \tag{66}$$

where we have used the summation by parts identity, equation (63). By the principle of virtual work, we also have

$$dE = -\sum_{\mathbf{q}\in\mathcal{Q}_h} f_i dX_i (\alpha h)^3, \tag{67}$$

and comparison of equations (66) and (67) shows that $f_i$ is indeed given by equation (64). Note that $-\mathbf{f}$ is the gradient of $E$ with respect to the discrete inner product defined by equation (57).

Equation (64) defines $\mathbf{f}$ in terms of the configuration $\mathbf{X}$ of the elastic material. During the computation, time proceeds in steps of duration $\Delta t$, and the question arises whether the configuration at the beginning or the end of the time-step (or perhaps some intermediate configuration) should be used to compute the force for the step. Of course, the most expedient choice is the initial configuration of the time-step, since it has the virtue of being known. The resulting numerical scheme is called explicit, since it involves an explicit formula for $\mathbf{f}$. The use of the final configuration of the time-step has the alternative virtue of enhancing the stability of the computational method (Ref. 17), but it requires the solution of a dense nonlinear system to find the unknown final configuration. A scheme based on this choice is called implicit, because the material configuration from which the elastic force is computed is only implicity defined. Here, we describe an approximately implicit scheme, in which an approximation to the final configuration is used at each step.

Let time proceed in steps of duration $\Delta t$, and let a superscript $n$ be the time-step index so that $\mathbf{X}^n(\mathbf{q}) = \mathbf{X}(\mathbf{q}, n\Delta t)$, and similarly for all other functions of time. Then the approximately implicit scheme for the computation of the elastic force may be stated as follows:

$$m\frac{\widetilde{\mathbf{X}}^{n+1} - 2\mathbf{X}^n + \mathbf{X}^{n-1}}{(\Delta t)^2} = \mathbf{f}^{n+1}, \tag{68}$$

$$f_i^{n+1} = \sum_{j=1}^{3} D_{q_j}^- \mathcal{E}_{ij}^{n+1}(D_{\mathbf{q}}^+ \widetilde{\mathbf{X}}^{n+1}, \mathbf{q}), \tag{69}$$

where $D_{\mathbf{q}}^+ \widetilde{\mathbf{X}}^{n+1}$ denotes the $3 \times 3$ matrix whose $kl$ entry is $D_{q_l}^+ \widetilde{X}_k^{n+1}$. Equations (68) and (69) constitute a nonlinear system in the unknowns $\widetilde{\mathbf{X}}^{n+1}(\mathbf{q}), \mathbf{f}^{n+1}(\mathbf{q})$. This system is solved by Newton's method. No further use is made of the approximate final configuration $\widetilde{\mathbf{X}}^{n+1}$, but $\mathbf{f}^{n+1}$ is used as the elastic force for the time-step from $t = n\Delta t$ to $t = (n+1)\Delta t$.

We remark that the scheme given by equations (68) and (69) is precisely the backward-Euler method for the numerical solution of the Langrangian equations of motion that one would get from the principle of least action by ignoring the constraint of incompressibility [see eq. (13)]. These equations are

$$m\frac{\partial^2 X_i}{\partial t^2} = f_i = \sum_{j=1}^{3} \frac{d}{dq_j}\mathcal{E}_{ij}. \tag{70}$$

The backward-Euler discretization of these equations has the effect of filtering out high-frequency components of the force that would otherwise de-stabilize the computation.

Finally, we consider the Eulerian variables, which satisfy the Navier-Stokes equations [eqs. (34)–(35)]. These equations are solved by Chorin's projection method (Refs. 18, 19) on the regular cubic lattice $\Omega_h$; the irregular geometry of the Lagrangian marker array plays no role at all in this part of the computation.

To state the projection method, we make use of the difference operators $D^{\pm}$ introduced above, and we also define

$$D^0 = \frac{1}{2}(D^+ + D^-) \tag{71}$$

$$\mathbf{D}^0 = (D^0_{x_1}, D^0_{x_2}, D^0_{x_3}). \tag{72}$$

Note that $\mathbf{D}^0$ is the vector difference operator corresponding to the vector differential operator $\nabla$.

The goal of the projection method is to compute $\mathbf{u}^{n+1}$ and $p^{n+1}$ given $\rho^n$, $\mathbf{u}^n$, and $\mathbf{F}^{n+1}$. This is accomplished in a series of implicit fractional steps in which several intermediate velocity fields are found. These are denoted $\mathbf{u}^{n+1,s}$, where $s = 1, 2, 3$. Then, in the last fractional step $\mathbf{u}^{n+1}$ and $p^{n+1}$ are computed. The equations to be solved are as follows:

$$\rho^n \frac{\mathbf{u}^{n+1,0} - \mathbf{u}^n}{\Delta t} = \mathbf{F}^{n+1}, \tag{73}$$

$$\rho^n \left( \frac{\mathbf{u}^{n+1,s} - \mathbf{u}^{n+1,s-1}}{\Delta t} + u^n_s D^0_{x_s} \mathbf{u}^{n+1,s} \right) = \mu D^+_{x_s} D^-_{x_s} \mathbf{u}^{n+1,s} \quad \text{for } s = 1, 2, 3, \tag{74}$$

$$\rho^n \frac{\mathbf{u}^{n+1} - \mathbf{u}^{n+1,3}}{\Delta t} + \mathbf{D}^0 p^{n+1} = 0, \tag{75}$$

$$\mathbf{D}^0 \cdot \mathbf{u}^{n+1} = 0, \tag{76}$$

[eqs. (75)–(76) should be regarded as a system in the unknowns $\mathbf{u}^{n+1}$, $p^{n+1}$]. To see the correspondence between the projection method and the Navier-Stokes equations, add equations (73)–(75) [keeping in mind that eq. (74) is really three separate equations]. Note that all intermediate velocity fields cancel out of the time-derivative term. The result is

$$\rho^n \left( \frac{\mathbf{u}^{n+1} - \mathbf{u}^n}{\Delta t} + \sum_{s=1}^{3} u^n_s D^0_{x_s} \mathbf{u}^{n+1,s} \right) + \mathbf{D}^0 p^{n+1} = \mu \sum_{s=1}^{3} D^+_{x_s} D^-_{x_s} \mathbf{u}^{n+1,s} + \mathbf{F}^{n+1}. \tag{77}$$

This is consistent with the first of the Navier-Stokes equations [eq. (34)] because $\mathbf{u}^{n+1,s}$ is within $O(\Delta t)$ of $\mathbf{u}^n$ or $\mathbf{u}^{n+1}$ for all $s$.

Equation (73) is a separate equation for each lattice point $\mathbf{x}$ of $\Omega_h$, so it is easily solved for $\mathbf{u}^{n+1,0}$.

For each $s$, equation (74) has coupling only in the $x_s$ direction. Moreover, this coupling is only between a point and its nearest neighbors. Thus, equation (74) amounts to a tridiagonal system for each row (when $s = 1$), for each file (when $s = 2$), or for each column (when $s = 3$) of $\Omega_h$. These systems are linear because $\rho^n$ and $\mathbf{u}^n$ are known. [Note that $\mathbf{u}^n = (u^n_1, u^n_2, u^n_3)$ is always used as the convection velocity.]

Equations (75) and (76) constitute a system in the unknowns $\mathbf{u}^{n+1}$, $p^{n+1}$. This

pair of equations can be reduced to a single Poisson equation for the pressure

$$\mathbf{D}^0 \cdot \frac{1}{\rho^n} \mathbf{D}^0 p^{n+1} = \frac{1}{\Delta t} \mathbf{D}^0 \cdot \mathbf{u}^{n+1,3}. \tag{78}$$

Despite the appearance of $(\Delta t)^{-1}$, the right-hand side is $O(1)$ because $\mathbf{D}^0 \cdot \mathbf{u}^{n+1,3}$ is $O(\Delta t)$. In the important special case $\rho^n(\mathbf{x}) = \rho_0$, independent of $\mathbf{x}$, equation (76) has constant coefficients and may be solved by Fourier transform techniques. Otherwise, iterative methods are required (Ref. 20). Once the pressure is known, equation (75) is easily solved for $\mathbf{u}^{n+1}$.

We have now described all of the ingredients of the numerical method for the solution of equations (34)–(39). These ingredients are combined as follows.

At the beginning of a time-step, $\mathbf{X}^n$ and $\mathbf{u}^n$ are known. (The data $\mathbf{X}^{n-1}$ are also known from the previous step.) The goal of the method is to compute $\mathbf{X}^{n+1}$ and $\mathbf{u}^{n+1}$. The first step is to find the elastic force $\mathbf{f}^{n+1}$ by solving the nonlinear system.

$$m \frac{\widetilde{\mathbf{X}}^{n+1} - 2\mathbf{X}^n + \mathbf{X}^{n-1}}{(\Delta t)^2} = \mathbf{f}^{n+1}, \tag{79}$$

$$f_i^{n+1} = \sum_{j=1}^{3} D_{q_j}^- \mathcal{E}_{ij}^{n+1}(D_{\mathbf{q}}^+ \widetilde{\mathbf{X}}^{n+1}, \mathbf{q}). \tag{80}$$

At this point the Lagrangian mass and force densities $m$ and $\mathbf{f}^{n+1}$ are converted to Eulerian form:

$$\rho^n(\mathbf{x}) = \sum_{\mathbf{q} \in \mathcal{Q}_h} m(\mathbf{q}) \delta_h^3[\mathbf{x} - \mathbf{X}^n(\mathbf{q})](\alpha h)^3, \tag{81}$$

$$\mathbf{F}^{n+1}(\mathbf{x}) = \sum_{\mathbf{q} \in \mathcal{Q}_h} \mathbf{f}^{n+1}(\mathbf{q}) \delta_h^3[\mathbf{x} - \mathbf{X}^n(\mathbf{q})](\alpha h)^3. \tag{82}$$

Equations (81) and (82) hold for all $\mathbf{x} \in \Omega_h$. In both of these equations, the argument of $\delta_h^3$ involves the initial configuration $\mathbf{X}^n$ rather than the approximate final configuration $\widetilde{\mathbf{X}}^{n+1}$. With $\rho^n$ and $\mathbf{F}^{n+1}$ determined, we proceed to the solution of the Navier-Stokes equations: First set

$$\mathbf{u}^{n+1,0} = \mathbf{u}^n + \frac{\Delta t}{\rho^n} \mathbf{F}^{n+1}. \tag{83}$$

Then solve successively the following systems, in which the unknown in each case is $\mathbf{u}^{n+1,s}$, for $s = 1, 2, 3$:

$$\rho^n \left( \frac{\mathbf{u}^{n+1,s} - \mathbf{u}^{n+1,s-1}}{\Delta t} + u_s^n D_{x_s}^0 \mathbf{u}^{n+1,s} \right) = \mu D_{x_s}^+ D_{x_s}^- \mathbf{u}^{n+1,s}, \tag{84}$$

Next, find the pressure by solving the (variable-coefficient) Poisson equation

$$\mathbf{D}^0 \cdot \frac{1}{\rho^n} \mathbf{D}^0 p^{n+1} = \frac{1}{\Delta t} \mathbf{D}^0 \cdot \mathbf{u}^{n+1,3}, \tag{85}$$

and evaluate $\mathbf{u}^{n+1}$ as follows

$$\mathbf{u}^{n+1} = \mathbf{u}^n - \frac{\Delta t}{\rho^n}\mathbf{D}^0 p^{n+1}. \tag{86}$$

Finally, move the elastic material according to the formula

$$\mathbf{X}^{n+1}(\mathbf{q}) = \mathbf{X}^n(\mathbf{q}) + \Delta t \sum_{\mathbf{x}\in\Omega_h} \mathbf{u}^{n+1}(\mathbf{x})\delta_h^3[\mathbf{x} - \mathbf{X}(\mathbf{q})]h^3, \tag{87}$$

which holds for all $\mathbf{q} \in \mathcal{Q}_h$. Since the velocity and configuration have been updated, this completes the time-step.

## 4. Application: the heart

The purpose of this section is to give an example which illustrates the mathematical formulation and numerical method described above. The example we choose is the heart.

Cardiac muscle is an incompressible elastic material which (to a reasonable approximation) is neutrally buoyant in blood. The elastic parameters of cardiac muscle are strongly time-dependent; it is this explicit dependence of the elastic parameters on time that makes the heart beat (Ref. 21).

Another important property of cardiac muscle is its anisotropy. The muscle is organized in such a way that there is a definite fiber direction at each point. The fiber direction varies continuously as a function of position in the heart wall. For empirical descriptions of the fiber architecture of the heart, see References 22–24; a mathematical theory which explains some observed features of the fiber architecture has also been developed (Refs. 24, 25).

Consider, then, an elastic material made of fibers in which the elastic energy density depends only on the strain in the fiber direction. Let the curvilinear coordinates $q_1$, $q_2$, and $q_3$ be chosen in such a way that $q_2$ and $q_3$ are constant along the fibers. Then the fiber strain is determined by $|\partial\mathbf{X}/\partial q_1|$, and the elastic energy is of the form

$$\mathcal{E} = \bar{\mathcal{E}}(|\partial\mathbf{X}/\partial q_1|, \mathbf{q}, t). \tag{88}$$

It follows that

$$\mathcal{E}_{ij} = \frac{\partial\mathcal{E}}{\partial(\partial X_i/\partial q_j)} = 0 \quad \text{for} \quad j \neq 1, \tag{89}$$

while

$$\mathcal{E}_{i1} = \frac{\partial X_i/\partial q_1}{|\partial\mathbf{X}/\partial q_1|}\bar{\mathcal{E}}'(|\partial\mathbf{X}/\partial q_1|, \mathbf{q}, t), \tag{90}$$

where $\bar{\mathcal{E}}'$ denotes the derivative of $\bar{\mathcal{E}}$ with respect to its first argument. To derive equation (90) (an exercise which we leave to the reader), it is helpful to write out $|\partial\mathbf{X}/\partial q_1|$ as follows:

$$\left|\frac{\partial\mathbf{X}}{\partial q_1}\right| = \left[\sum_{k=1}^{3}\left(\frac{\partial X_k}{\partial q_1}\right)^2\right]^{1/2}. \tag{91}$$

Note that $\mathcal{E}_{i1}$ is the $i$ component of a vector which may be denoted $T\tau$ where

$$\tau = \frac{\partial \mathbf{X}/\partial q_1}{|\partial \mathbf{X}/\partial q_1|} \tag{92}$$

is the unit tangent to the fibers, and where

$$T = \bar{\mathcal{E}}'(|\partial \mathbf{X}/\partial q_1|, \mathbf{q}, t) \tag{93}$$

is the fiber tension in the sense that $T\,dq_2\,dq_3$ is the force transmitted by the bundle of fibers $dq_2\,dq_3$.

According to equation (80), the Lagrangian elastic force density $\mathbf{f}$ is given by $f_i = \sum_{j=1}^{3} d\mathcal{E}_{ij}/dq_j$. In our case, only the first term in the sum is nonzero, so $f_i = d\mathcal{E}_{i1}/dq_1$, or

$$\mathbf{f} = \frac{d}{dq_1}(T\tau). \tag{94}$$

For an alternative derivation of equation (94), see Reference 8.

Equations (92)–(94) are discretized as follows:

$$\tau = \frac{D_{q_1}^{+}\mathbf{X}}{|D_{q_1}^{+}\mathbf{X}|}, \tag{95}$$

$$T = \bar{\mathcal{E}}'(|D_{q_1}^{+}\mathbf{X}|, A_{q_1}^{+}\mathbf{q}, t), \tag{96}$$

$$\mathbf{f} = D_{q_1}^{-}(T\tau). \tag{97}$$

In equation (96), we have exploited the one-dimensional character of the fibers by replacing $\mathbf{q}$ by $A_{q_1}^{+}\mathbf{q}$, where $A_{q_1}^{+}$ is the forward averaging operator defined by

$$(A_{q_1}^{+}\phi)(q_1, q_2, q_3) = \frac{1}{2}[\phi(q_1 + \alpha h, q_2, q_3) + \phi(q_1, q_2, q_3)]. \tag{98}$$

Thus,

$$A_{q_1}^{+}\mathbf{q} = (q_1 + \frac{\alpha h}{2}, q_2, q_3). \tag{99}$$

This shift provides centering that makes equations (95)–(97) a second-order accurate discretization of equations (92)–(94), despite the formal first-order accuracy of the forward and backward difference operators. To make this second-order accuracy evident, think of the variables $T$ and $\tau$ as being associated with the links between marker points instead of with the markers themselves. Then equations (95) and (96) provide second-order accurate values of $\tau$ and $T$ at the points $(q_1 + \frac{\alpha h}{2}, q_2, q_3)$, and equation (97) provides a second-order accurate value of $\mathbf{f}$ at $(q_1, q_2, q_3)$.

The foregoing discussion applies to any elastic material made of fibers in which there is a definite fiber direction at each point and in which the elastic energy density depends only on the strain in the fiber direction. To specify a model of the heart, one must also say how the fibers are arranged in space. This is done according to the following principles:

1. We set up a specific arrangement of cardiac muscle fibers that will be used as the initial configuration of the model heart. This configuration is intended to

model the heart at the beginning of diastole, which is the phase of the cardiac cycle in which the ventricles relax and fill with blood. If the model heart is run through several cycles, however, it will eventually find its own periodic steady state, and there is no reason for it ever to return to the precise configuration that we specify at time zero. Thus, the configuration that we specify determines the dynamic anatomy of the model heart, but only indirectly.

2. According to Thomas, cardiac muscle fibers begin and end at the valve rings (Ref. 22). There are four such rings, one for the inflow valve and one for the outflow valve on each side of the heart. These rings are roughly coplanar, and the plane that (more or less) contains them is called the base of the heart. In the initial configuration of the model, the valve rings are actually coplanar. Each fiber of the model heart is a closed-space curve which begins at some point on one of the valve rings, follows some path through space that eventually arrives at a (possibly different) valve ring, and then closes on itself by running along the rings themselves and along certain straight-line connections that make possible smooth transitions from one ring to another.

3. According to Streeter et al., the cardiac muscle fibers of the left ventricle are geodesics (curves of shortest length) on a nested family of toroidal surfaces in the interior of the left ventribular wall (Ref. 24). We exploit this observation by specifying surfaces rather than individual fibers. Once the surfaces have been specified, the geodesic fiber paths are determined merely by specifying an initial point and direction for each fiber. For some of the surfaces that we use, the geodesic fiber paths can be determined analytically, but in any case they can be found numerically.

Further details concerning the construction of the model heart are shown in Figure 1. Overall, it contains left and right ventricles; left and right atria; the mitral, tricuspid, aortic, and pulmonic valves; and segments of the following great-vessels: the aorta, the main pulmonary artery, the superior and inferior vena cavae, and the four pulmonary veins. The model great-vessels have blind ends, but these are equipped with sources and sinks which connect the model heart to a simulated circulation. (Since the pulmonary veins are small, we use a single source in the left atrium instead of a separate source in each pulmonary vein.) The computational apparatus needed to specify sources and sinks is described in Reference 2.

Once the anatomy of the model heart has been specified, its physiology can be determined by postulating a stress-strain law for its elastic fibers and especially by stipulating the position- and time-dependence of the elastic parameters that appear in that constitutive equation. We use a two-parameter stress-strain law, the parameters being the stiffness and the resting length. For valves and great-vessels, these parameters are constant, but for the atria and ventricles they are functions of time. At present, we vary these parameters synchronously throughout the atria and synchronously throughout the ventricles, but with different time-dependence in the atrial case and in the ventricular case. Thus, we

do simulate the time-delay between the atrial contraction and the ventricular contraction, but we do not (as yet) simulate the wave-like character of the contraction within the atria or within the ventricles. This is a refinement that can be made later.

Some results of our computations are shown in Figure 2. The snapshots of the flow patterns are made by taking a thick cross section of the model and recording the trajectories of fluid particles within that cross section over several time-steps. (Each particle is shown as a dot in its current position with a tail showing its recent trajectory.)

These computations are preliminary; the three-dimensional heart model described here has not yet been put to use. Ultimately, we hope that it will be used for improved understanding of normal cardiac function, for computer modeling of diseases affecting the mechanical function of the heart or its valves, and for computer-assisted design of prosthetic cardiac valves. All three of these potential applications have already been realized in the case of a two-dimensional heart model developed earlier (e.g. Refs. 4–7).

## 5. Conclusion

A general method for the numerical solution of problems in which an incompressible fluid interacts with an incompressible elastic material has been described. Since most problems of biofluid dynamics are of this type, the method has broad applicability.

A particular strength of the method described here is its geometric versatility. The geometry of the elastic material can be complicated, time-dependent, and unknown (since it is determined as part of the solution of the problem). This versatility arises from the use of a mixed Lagrangian-Eulerian description of the motion. The Lagrangian description is used to compute elastic forces, which are then transferred to the Eulerian computational lattice, on which the discretized Navier-Stokes equations are solved. The computed Eulerian velocity field is then used to update the Lagrangian configuration of the elastic material. The transfer of information in either direction between the Eulerian and Lagrangian descriptions is mediated by an approximation to the Dirac delta function.

The method is here illustrated by its application to the heart, but this conference has seen the presentation of a broad array of fascinating phenomena, ranging from filter feeding to bird flight and to which the method should be adaptable. Most of these problems seem too complex for further theoretical progress along purely analytic lines, but the method of this paper offers the hope that computer simulations of such complex phenomena are not out of reach.

## References

1. Peskin, C. S.: Flow Patterns around Heart Valves: A Digital Computer Method for Solving the Equations of Motion. Albert Einstein College of Medicine, Yeshiva University, New York, July 1972.

2. Peskin, C. S.: Numerical Analysis of Blood Flow in the Heart. J. Comput. Phys., vol. 25, 1977, pp. 220–252.
3. Peskin, C. S.; and McQueen, D. M.: Modeling Prosthetic Heart Valves for Numerical Analysis of Blood Flow in the Heart. J. Comput. Phys., vol. 37, 1980, pp. 113–132.
4. McQueen, D. M.; Peskin, C. S.; and Yellin, E. L.: Fluid Dynamics of the Mitral Valve: Physiological Aspects of a Mathematical Model. Am. J. Physiol., 242, 1982, pp. H1095–H1110.
5. McQueen, D. M.; and Peskin, C. S.: Computer-Assisted Design of Pivoting-Disc Prosthetic Mitral Valves. J. Thorac. Cardiovasc. Surg., vol. 86, 1983, pp. 126–135.
6. McQueen, D. M.; and Peskin, C. S.: Computer-Assisted Design of Butterfly Bileaflet Valves for the Mitral Position. Scand. J. Thor. Cardiovasc. Surg., vol. 19, 1985, pp. 139–148.
7. Meisner, J.S.; McQueen, D.M.; et al.: Effects of Timing of Atrial Systole on LV Filling and Mitral Valve Closure: Computer and Dog Studies. Am. J. Pysiol., vol. 249, 1985, pp. H604–H619.
8. Peskin, C. S.; and McQueen, D. M.: A Three-Dimensional Computational Method for Blood Flow in the Heart: (I) Immersed Elastic Fibers in a Viscous Incompressible Fluid. J. Comput. Phys., vol. 81, 1989, pp. 372–405.
9. McQueen, D. M.; and Peskin, C. S.: A Three-Dimensional Computational Method for Blood Flow in the Heart: (II) Contractile Fibers. J. Comput. Phys., vol. 82, 1989, pp. 289–297.
10. Beyer, R. P.: A Computational Model of the Cochlea Using the Immersed Boundary Method. J. Comput. Phys., vol. 98, 1992, pp. 145–162.
11. Fauci, L. J.; and Peskin, C. S.: A Computational Model of Aquatic Animal Locomotion. J. Comput. Phys., vol. 77, 1988, pp. 85–108.
12. Fauci, L. J.: Interaction of Oscillating Filaments: A Computational Study. J. Comput. Phys., vol. 86, 1990, pp. 294–313.
13. Fauci, L. J.; and Fogelson, A. L.: Truncated Newton Methods and the Modeling of Complex Immersed Elastic Structures. Commun. Pure and Appl. Math., in press.
14. Fogelson, A. L.: A Mathematical Model and Numerical Method for Studying Platelet Adhesion and Aggregation during Blood Clotting. J. Comput. Phys., vol. 56, 1984, pp. 111–134.
15. Fogelson, A. L.: Mathematical and Computational Aspects of Blood Clotting. Proceedings of the 11th IMACS World Congress on System Simulation and Scientific Computation, Vol. 3, B. Wahlstrom, ed., North Holland, New York, 1985, pp. 5–8.

16a. Ebin, D. G.; and Saxton, R. A.: The Initial-Value Problem for Elastodynamics of Incompressible Bodies. Arch. Rat. Mech. Anal, vol. 94, 1986, pp. 15–38.

16b. Ebin, D. G.; and Saxton, R. A.: The Equations of Incompressible Elasticity. Contemp. Math., vol. 60, 1987, pp. 25–34.

17. Tu, C.; and Peskin, C. S.: Stability and Instability in the Computation of Flows with Moving Immersed Boundaries: A Comparison of Three Methods. SIAM J. Sci. Stat. Comput., in press.
18. Chorin, A. J.: Numerical Solution of the Navier-Stokes Equations. Math. Comp., vol. 22, 1968, pp. 745–762.
19. Chorin, A. J.: On the Convergence of Discrete Approximations to the Navier-Stokes Equations. Math Comp., vol. 23, 1969, pp. 341–353.
20. Adams, J. C.: MUDPACK: Multigrid Portable FORTRAN Software for the Efficient Solution of Linear Elliptic Partial Differential Equations. Appl. Math. Comput., vol. 34, 1989, pp. 113–146.
21. Sagawa, K.; Suga, H.; and Nakayama, K.: Instantaneous Pressure-Volume Ratio of the Ventricle versus Instantaneous Force-Length Relation of Papillary Muscle. Cardiovascular System Dynamics, J. Baan, A. Noordegraaf, and J. Raines, eds., M. I. T. Press, Cambridge, Mass., 1978, pp. 99–105.
22. Thomas, C. E.: The Muscular Architecture of the Ventricles of Hog and Dog Hearts. Am. J. Anatomy, vol. 101, 1957, pp. 17–57.

23. Streeter, D. D., Jr.; Spotnitz, H. M.; Patel, D. P.; Ross, J., Jr.; and Sonnenblick, E. H.: Fiber Orientation in the Canine Left Ventricle during Diastole and Systole. Circ. Res., vol. 24, 1969, pp. 339–347.
24. Streeter, D. D., Jr.; Powers, W. E.; Ross, M. A.; and Torrent-Guasp, F.: Three-Dimensional Fiber Orientation in the Mammalian Left Ventricular Wall. Cardiovascular System Dynamics, J. Baan, A. Noordegraaf, and J. Raines, eds., M. I. T. Press, Cambridge, Mass., 1978, pp. 73–84.
25. Peskin, C. S.: Fiber Architecture of the Left Ventricular Wall: An Asymptotic Analysis. Commun. Pure and Appl. Math., vol. 42, 1989, pp. 79–113.

Courant Institute of Mathematical Sciences, New York University, 251 Mercer Street, New York, New York 10012.

FIGURE 1. Fiber architecture of the model heart. (A) Construction of the left ventricular wall. At left, a double-sheeted layer of left ventricular fibers with the aortic and mitral valve rings at the top. There is space between the two sheets for other layers of fibers which are nested there. Fibers begin and end at the valve rings. They make a smooth transition from one sheet to the other at the lower ring in the figure. Middle, a larger layer of the same type. At right, the two layers shown together with the smaller one nested between the sheets of the larger. (B) The mitral and aortic valves. At left, a layer of fibers which surrounds both ventricles, penetrates the left ventricular wall at the apex of the heart, and returns to the valve rings via the inner surface of the left ventricular wall. Middle, the mitral valve, including chordae tendineae and papillary muscles, and the aortic valve, including the root of the aorta. At right, the mitral and aortic valves installed in the model heart. (C) Relation of the right and left ventricles. At left, the left ventricle with the mitral and aortic valves in place. Middle, the right ventricle has been added. At right, the model ventricles with all four valves in place. (D) Inflow structures. At left, the model ventricles. Middle, the atria, veins, and atrioventricular valves. At right, the inflow structures and the ventricles shown together. See pages 184 and 185.

FIGURE 2. The model heart in action. Top row: filling. Bottom row: ejection. In both rows the frame at left shows the fibers (atria and veins deleted for clarity), whereas the middle and right frames show selected cross sections of the flow pattern. Flow is visualized in terms of streak lines with a dot showing the current position and a tail showing the recent trajectory. See page 186.

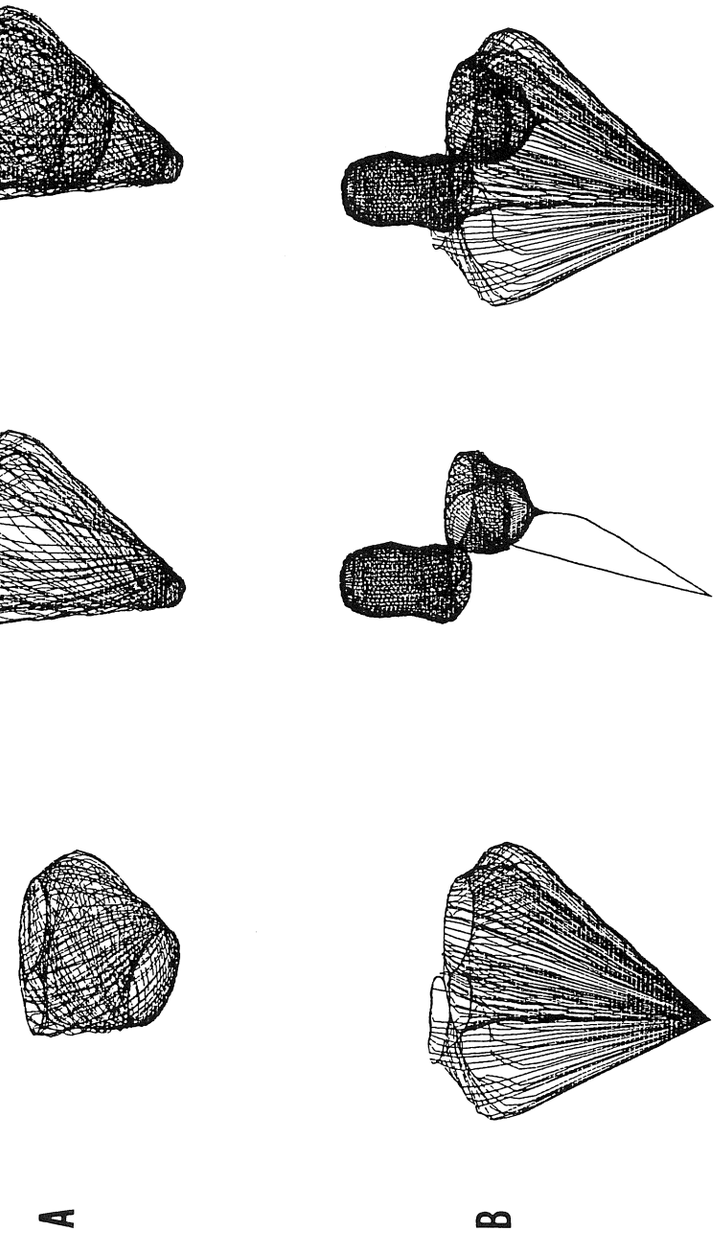


FIGURE 1.

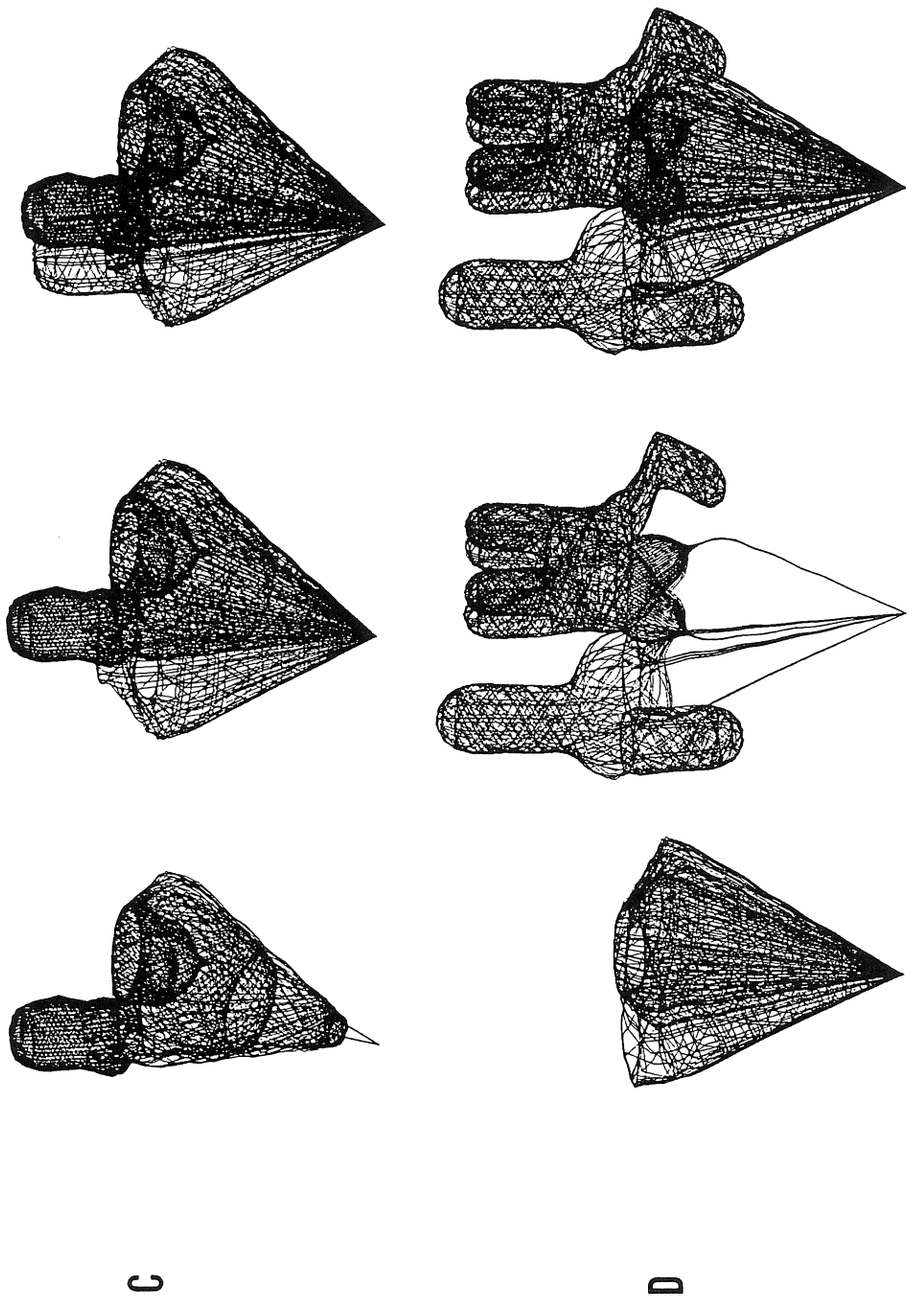


FIGURE 1.

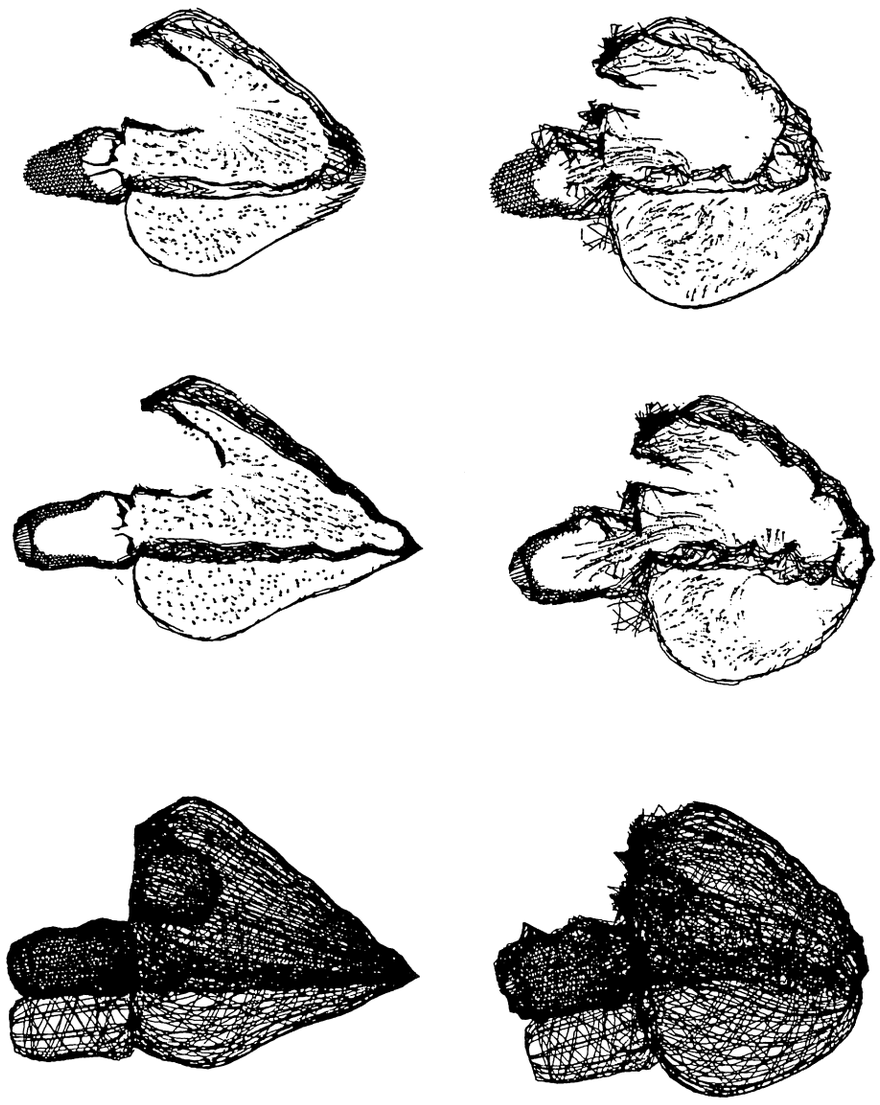

FIGURE 2.